WJCMS

Wasit Journal of Computer and Mathematics Science

Journal Homepage: https://wjcm.uowasit.edu.iq/index.php/WJCM
e-ISSN: 2788-5879 p-ISSN: 2788-5887

Brain Tumor Classification of Medical Images based on Transfer Pre-trained Learning Models

Mohamed H Ghaleb Abdkhaleq[1,*], Ibraheem Al-Jadir [2], Loay E. George[3], Gromov, Yuri Yuryevich[4], Eliseev Aleksey Igorevich[5]

[1]College of Computer Science and Information Technology, University of Wasit, Kut, Iraq.

[2]Ministry of higher education and scientific research, Baghdad, Iraq.

[3]College of Science, University of Baghdad, Baghdad, Iraq.

[4,5]Tambov State Technical University, Tambov, Russia.

*Corresponding Author: Mohamed H Ghaleb Abdkhaleq

DOI: https://doi.org/10.31185/wjcms.388
Received 31 May 2025; Accepted 25 June 2025; Available online 30 June 2025

ABSTRACT: Identifying brain tumor types is crucial for accurate diagnoses and appropriate therapeutic planning in medical imaging. The study aims to develop a robust and accurate system for categorizing medical images of brain tumors, utilizing transfer learning from pre-trained neural network models. The purpose is to optimize the efficiency and precision of brain tumor diagnosis, ultimately facilitating prompt and precise medical intervention by clinicians. This endeavor holds immense importance in promptly diagnosing and treating brain tumors. Transfer learning greatly facilitates the classification of different forms of brain tumors visible in medical imaging, enabling the achievement of this target. Utilizing pre-trained neural network models capitalizes on their comprehension of visual attributes and patterns by adjusting to the specific activity with efficiency and accuracy. Through this strategy, the training process is accelerated, and the model is generalized. Medical professionals can rapidly and reliably diagnosing brain tumors from medical imaging via this technique. he results demonstrate that the AlexNet model showed a remarkable performance, with an accuracy rate of 95.60% and high sensitivity and specificity rates.

Keywords: Tumor detection, Brain Tumor Detection, GLCM, CNN, Alex Net, Transfer Learning.

1. INTRODUCTION

With approximately 100 billion nerve cells, the mind is a complicated bodily component in the human body which controls the whole sensory system [1]. The sensory system's focal point is where this essential organ started. Any anomaly that occurs in this area could endanger people's health in this way. Brain tumors are the most dangerous of these abnormalities. Secondary and primary tumors are the two categories of brain tumors, which are the result of unnatural and uncontrolled cell development within the organ. The first form of tumors is found in the cerebrum, whereas the second type enters the cerebrum through the circulatory system after emerging from other areas of the body [2]. Gliomas and meningiomas are two of the most lethal types of primary tumors that can cause mortality if they are not detected early on [3]. Gliomas are really the most well-known type of brain tumor in humans [4]. The WHO has classified cerebrum cancers into four classes [1]. Grades 1 and 2 represent benign tumors (meningioma, for example), whereas grade 3 and grade 4 represent malignant tumors (glioma, for example). Pituitary, meningioma, and glioma tumor rates in clinical practice are approximately 15%, 15%, and 45%, respectively.

Deep learning (DL) is an Artificial Intelligence (AI) methodology which is considered as a Neural Network (NN) application that deals with complex data. With regard to architecture, DL networks and traditional NNs are comparable. That is to say, both feature the hidden layers, input layer, and output layer as structural elements. Nonetheless, compared to traditional NNs, there are more hidden layers in the DL case. When it comes to medical imaging, it becomes necessary to be using some intelligent methods such as the deep learning method to handle the complex patterns in these images and analyze them accurately. Medical imaging means the techniques and procedures utilized for creating images of different parts of the body to diagnose the illnesses in these images to find

the appropriate treatment according to the detected issue. Medical image includes several radiological imaging processes, including fluoroscopy, radiography, computed tomography (CT) scans, magnetic resonance imaging (MRI), and X-rays. The use of deep learning methods in different analytical processes related to medical images has successfully been suggested by research in various medical imaging applications. A lot of research has been conducted to provide accurate and precise solutions to classify brain tumor images automatically. Nonetheless, because of the high intra- inter shape, textures, and contrasts differentiations; it becomes an NP-Hard problem. The conventional machine learning (ML) tools depend on handcraft features that are restraining the powerfulness of the Solutions while the deep learning methods can be extracting optimal features in an automatic manner that could be offering potentially better outcomes but such techniques need quantities of dedicated data for training, and obtain this kind of data is challenging task [5].

A significant approach in ML, uses the strength of pre-trained neural network (NN) models to handle various tasks effectively. Its significance comes from its capacity to improve data use, boost generalization, save time and computing power, and provide better model performance. This technique has turned into a crucial part for getting top-notch outcomes in computer vision fields, natural language processing and others. It is an essential instrument in the toolbox of ML and AI.

The aim of the study is to create a strong and precise system for sorting medical images of brain tumors, using TL from pre-trained NN models. The goal is to enhance the speed and accuracy in diagnosing brain tumors, with an ultimate objective of aiding doctors in offering quick and accurate medical attention to patients. This task assumes a very high significance for fast brain tumor identification and treatment. Transfer learning has a highly significant impact on making possible this objective of the classification of various brain tumor types that can be seen in the medical images. With the use of pre-trained NN models, it takes advantage of their understanding in visual characteristics and patterns. This makes adapting to the particular task efficient and precise. Such method quickens training, improves model generalization, and assists medical experts to make brain tumor diagnosis from medical images swiftly and accurately.

The sections that follow are arranged as follows: The preliminary information is covered in part 2, the related work is covered in Section 3, the methodology is explained in depth and the findings are shown in Sections 4 and 5, and the conclusions are summarized in the last part.

2. RELATED WORK

In this section we present the most relevant related works associated with the suggested method in this paper. First the medical images processing techniques are reviewed and then the applications of the medical imaging have been highlighted too.

2.1 MEDICAL IMAGE PROCESSING TECHNIQUES

The set of methods that are used in order to create images of the body's internal organs for scientific and medical reasons is known as medical imaging. Additionally, it offers a visual representation of how inside tissues function. Diseases affecting the body's internal organs can be detected and treated with the help of medical imaging. In order to make the identification of anomalies easier, this method creates data banks with the typical functions and structures of the bodily components. This procedure includes both organic and radiological imaging, using thermos energies, sonographies, isotope imaging, scopes, magnetics, and electromagnetic radiation like gamma and X-rays. There are numerous more methods used to capture data about the functional and spatial characteristics of the body. These methods have certain limitations when compared to systems that generate images. Generally, billions of images are processed each year for various diagnostic uses. Ionizing as well as nonionizing radiation treatments are used by about half of them [8]. Without requiring surgery, medical imaging gene rates images of the body's internal architecture. Fast processing and arithmetical and logical conversions of the energy amounts to signal were used to produce those images [9]. After that, the signals are converted into digital representations that depict the many types of bodily tissues.

The advanced digital represents an essential part of the daily routine. The clinical imaging prepares the image to make it ready for further processing by the PC. This involves incorporating numerous sorts of strategies and tasks, such as picture acquiring, filtering, displaying, and transmission. The image is a representation that refers to the proportion of qualities such as light intensities, shading and illumination. Digital imaging has many advantages: quicker and modest handling cost, simple putting away and correspondence, prompt quality evaluation, various duplicating with saving the quality, quick and modest generation, and versatile control.

Using a computer for editing digital images has been referred to as image processing. Numerous advantages of this approach include communication, flexibility, data storage, and adaptability. The development of various methods of image scaling had made it possible maintaining images in an effective manner. Numerous sets of criteria have to be applied in a simultaneous manner to images in this method. Multiple dimensions could be handled for 3D as well as 2D images. The 1960s saw the invention of image processing technology. These approaches have been applied in various

sectors, which include space exploration, medicine, arts, and enhancement of TV images. The cost and speed of image processing decreased throughout the 1970s as computer systems advanced. Image processing got easier, cheaper, and faster in the 2000s [11].

2.2 APPLICATIONS OF MEDICAL IMAGING

One application that needs AI techniques is medical imaging analysis. Numerous researchers have experimented with various methods to address a variety of pre- and post-processing-related problems in medical image analysis. A wealth of useful information on abnormal and normal patterns in these kinds of images may be found in the medical images. The most widely used tests for diagnosis that confirm the existence of any aberration, including abnormalities or tumors, are endoscopy, MRI, and CT imaging. These images essentially combine examples of both abnormal and normal images. The identification and classification of image defects remain one of the most active and hard study fields even with extensive research in this domain. The technologies of digital image analysis have a notable effect in the detection of specific illnesses in medical applications. With the widespread of combining the digital image with Web, a wide range of improvements in health protections has been made [12]. Different techniques are used in this field: noise detections, noise eliminations, watermark incorporation, feature extracting, image segmenting, and image compressing. In this review, we discuss the use of the Genetic in all these applications.

Nematzadeh, Hossein; et al. [7], the authors suggest a hybrid model of coupled map lattices as well as Modified Genetic Algorithm (MGA) for encrypting medical images. To create the initial population of MGA, the suggested technique first uses a coupled map lattice to construct the number of secure cypher images. It then uses the MGA to reduce computational algorithm time and raise cypher-image entropy. Computer simulations and experimental findings show that the hybrid algorithm-based suggested approach has good encryption performance and can withstand a variety of common attacks.

Arif, Muhammad [8], a novel fusion method for multi-modal medical images has been presented. It was based upon curvelet transform as well as genetic algorithm (GA). By using GA in this way, one may eliminate any doubts and disperse any existing information in the input image, all while further optimizing the features of image fusion. The well frequency disintegrations were performed using curvelet transform. For the purpose of optimizing features, curvelet transformation is used to reform the GA fitness function. In addition, a new wrapper approach was applied to combine the how- and high-frequencies of the curvelet coefficient. We used discrete ridge-let transforms to examine each image structure independently. Curvelet transformation probability as well as the superposition approach have been defined. The flat areas of the original input medical imaging data were made clear and unambiguous using the GA. In addition, GA was utilized for optimizing the feature for image fusions in order to accomplish quick calculation times. Copulas and GA are used for integrating the raised output of the 2 images and obtain the high-frequency curvelet constant regarding the basis images. With the use of FS, FF, and copulas distributions, the new high and low frequencies of curvelet coefficients for fused images have been selected from input image.

Wang, Guojun [9], methods depending on modified GA were suggested for the classification of MR brain images. In this paper, three different GA approaches were proposed for feature selection. For all of the GA-based techniques, the classifier was Back Propagation Neural BPN. The recommended methods outperformed the conventional GA-based technique in accuracy by an estimated 4% to 6%. The quantity of features in these suggested features was decreased in addition to their increased accuracy. As a result, the system's complexity will decrease. As a result, the suggested methods had a notable improvement in performance metrics.

Hemanth, D. Jude [10], studied the performance of enhanced tumour detection, the authors examined the comparison method of several segmentation approaches and, in their study, compared their segmentation scores to determine the best. The GA is used for the automatic classification regarding tumor stage in order to increase classification accuracy. Area calculation as well as the extraction of pertinent features enhance the classification stage decision. The quality analysis and performance of MRI images using the suggested method's experimental findings are assessed and validated depending on the score of segmentation, sensitivity, and the other evaluation criteria that quantifies the accuracy percentages. The experiment's outcomes, which included average score of segmentation between 0.82 and 0.93, 92.03% accuracy, 92.36% sensitivity, and 91.42% specificity, showed how well the suggested method worked for differentiating between normal and pathological tissues in brain MR images.

In [11], Anitha, J., in order to automatically optimize network architectures, the authors proposed a GA-based network evolution method that looks for the fittest genes. Through TL and an experience-based, greedy exploration strategy, they accelerated the evolutionary process. Because of the evolutionary algorithm's procedural flexibility, it is possible to find potential NNs by utilizing state-of-the-art modules (such as the residual blocks). They assessed the framework using denoising, a standard task in medical image processing. The Computed Tomography Perfusion (CTP) image denoising experimental results show that the approach can be used to find the best genes to construct high-performance networks, or EvoNets.

Bahadure and et al. [12] proposed novel approach built on the basis of the Genetic Algorithms for gray scale. Various processes (initialization, mutation, and crossover) incorporated in the algorithm. The test outcomes obtained from the rigor security analyses (correlated coefficients, entropies, NPCRs, keys sensitivity, MSEs, etc.) proved the powerfulness of the suggested method and showed that the suggested has a high order of protection and therefore it

might be utilized for synchronizing the transmission of digital grayscale medical image. Summary of the methods reviewed in this paper.

Liu, Peng; et al. [13], the authors suggested using Optimum Homomorphic Wavelet Fusion (OHWF) to combine multi-modular clinical images. In this case, the advantages of homomorphic channel as well as wavelet transformation are integrated into a single image outline. The suggested approach improves the combination's nature by combining functional and anatomical features through staggered disintegration. For several information-based images, we executed MR-PET, MR T1-T2, MR-SPECT, and MR-CT modular combinations here. In order to apply Hybrid Genetic – Gray Wolf Optimization (HG-GWO), the optimal scale esteems are selected. The arbitrary control boundaries in HG-GWO are optimally selected by hereditary computation. In terms of MI, *QABF/* STD, and entropy value, OHWF is compared with various combination approaches for the execution assessment. It is found that compared to other condition of craftsmanship improvement processes, the combination effects of our suggested method are more pronounced. The staggered disintegration combination, obtained using our approach, has greater importance in clinical findings. The suggested OHWF technique uses a pixel-based combination; in future, portioned planning computations will be required to provide mechanized destruction of various neurological issues. In subsequent research, the suggested work can be used to determine the early stages of Alzheimer's disease infections and brain tumors using DL computations.

Pareek, N. K. and V. Patidar [14] , the authors suggested a recognition model regarding the irregularity in endoscopy NPC images, which is acknowledged on all endoscopy NPC images, in order to distinguish the typical cases (which only contain solid tissue) from the unusual cases (which The goal of this investigation was to identify irregularities in endoscopic NPC images and use that information to distinguish between conventional cases, which only included solid tissue, and rare ones, which included both dangerous and sound tissue. Pre-handling procedures are carried out using the endoscopic images that show non-NPC tissue extraction. The majority of the time, radiologists use visual screening to deconstruct the endoscopic images in order to identify and isolate any tumor-like or abnormalities existing in the texture captured from the images. This analysis demonstrates the novel method for distinguishing between normal and unusual tissue in nasopharyngeal endoscopic images. The three after advancements that comprise the suggested strategy are, first and foremost, Integral endoscopy images by measuring each pixel (x, y) in turn. Furthermore, train the ANN: determine the Positive's Haar highlight dread. Additionally, the following negative examples, which we have already altered, emphasize determination (GA): There are over 180,000 possible square shape highlights for a 24 by 24 location.

Mohammed, M. A. and et al. [15], in this article the authors trained the ANN by scanning the full image with different window sizes. To expedite the plan, the required image has re-registered for each window. The Haar has a number of channels. The testing stage made advantage of the highlights we generated from the GA during the preparation phase, and the locations were grouped using the prepared ANN. With a high 96.22% accuracy, 94.55% explicitness, and 95.35% affectability, the classifier performs well.

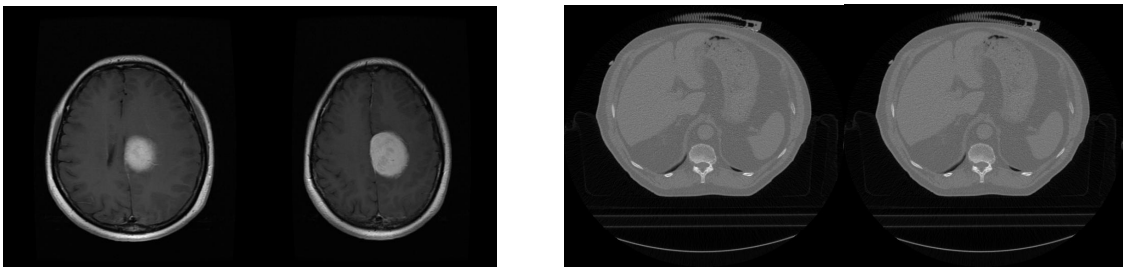

(a)Two examples of brain cancer images (b) Two examples of brain non-cancer images

Figure -1 Exemplary images showcasing normal brain anatomy in two distinct views (a) Two examples of brain cancer images (b) Frame 2.

3. GLCM-CNN BRAIN IMAGE CLASSIFICATION METHOD

This this section we explain the main steps used to design the proposed tumor image classification system using the GLCM and the CNN which can be represented as shown in the figure-2

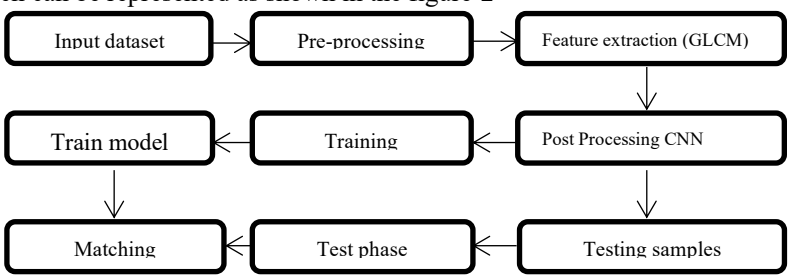

Figure -2 Systems framework

1. Image data quantization. Every echogram sample is viewed as a separate image pixel, and its intensity is represented by its sample value. After that, as described under Quantization, such intensities are further quantized to a predetermined number of the discrete grey levels.
2. Create GLCM. It will be a NxN square matrix, in which N represents the number of the levels that the quantization specifies. The following is how the matrix is made:
   a. Assuming that *s* is the sample that is considered for calculation.
   b. Assuming that *W* is the set of samples that surround *s* and fall within a window that is centered upon s of the size that has been specified under window Size.
   c. Considering only samples in *W*, every element *i,j* of GLCM is defined as the number of times 2 samples of intensities *i* and *j* occur in specified spatial relationship (where *i* & *j* represent the intensities between 0 and **No. of levels**-1). The summation of all elements (*i*, *j)* of GLCM will be total number of times the specified spatial relationship occurs in *W*.
   d. Make GLCM symmetric:
      i. Make a transposed GLCM copy,
      ii. Add that copy to actual GLCM.

   These lead to producing a symmetrical matrix where *i* to *j* relationship is not distinguishable for *j* to *i* relationship (for any 2 values of intensity *i* & *j*). Which is why, the summation of all elements (*i*, *j)* of GLCM will now be twice the total number of the times a specified spatial relationship occurs in *W* (once where sample with intensity *i* is the reference sample and the other time where the sample with the intensity *j* is the reference sample), and for any *i*, the summation of all elements *i*, *j* with given *i* will be the total number of the times an intensity *i* sample appears in specified spatial relationship with another sample.
   e. Normalize GLCM
   f. Divide every element by summation of all the elements of GLCM elements may now be viewed as probabilities of finding relationship *i*, *j* (or *j*, *i*) in *W*.
3. Calculate chosen feature.
4. The sample *s* in resulting virtual variable is substituted by this calculated feature's value.
5. The GLCM is applied as a method used for the feature's extraction. This method is responsible for extracting features from the image: contrast, correlation, energy, homogeneity, means, standard deviation, entropy, energy, RMS, variance, smoothness, kurtosis, and skewness.
   Thus, the total number of features extracted is 13, these features are extracted from each sample image in each dataset.
6. The convolutional neural network is applied next as a post-processing step. In order to setup the layers of the CNN the first thing is to construct the input layer which needs the feature vector to be in the format of [13 1 1] where the [x y z] format is used by the CNN. The convolutional matrix will be constructed as 3*12 which represents the size of the kernel, the RELU layer, and the FCL which is setup to be (2) as the number of classes. Last, the softmax is the activation function used for this network.
   The training is based on the following parameters:
   - The training options is based on the ADAM model.
   - Initial learning rate is 0.001.
   - Maximum epochs equal 100.
7. The last step is the validation process which is based on the idea of matching the input image samples to in an aim to be accurately classified according to the predicted error calculation at the classification process.

CNN steps

1. Convolution: The filtering process is carried out by the convolutional layer. The main component of ConvNet's learned weights during training are its convolutional layers. We refer to these scales as cores. The main function of the core is to generate a weighted pixel sum by scanning the image.
2. Activation Function: This is a NN's most crucial component. Based on the information it receives, the activation function determines whether or not a specific neuron will fire before sending it to the following layer. Because of its straightforward implementation and ability to overcome numerous challenges posed by other activation functions, like the Sigmoid, ReLU, is the most commonly utilized activation function.

Since the Softmax activation function is utilized for classifying datasets with many classes, we included it in the model as well.

3. Maxpooling: In the convolutional process known as "max pooling," the kernel retrieves maximum value from the region that it covers. We could utilize average pooling, just as max pooling. We would like to reduce function map to retain just the most useful portion of ReLU (Detect) function because function map ends up with a lot of "dead space."

To recap, the first step is the input and the pre-processing step where the training images are input to the system. The input dataset is used which are 224 this number is composed of 114 normal brain images and another 114 that represents cancerous image of the brain. When it comes to the testing data. 28 images for the normal test images and 28 for the cancerous image sample. The supervised system training is used to label two classes 1 for the normal image classes and 2 for the cancerous one. Thus, the above steps can be classified into the steps shown in figure-3.

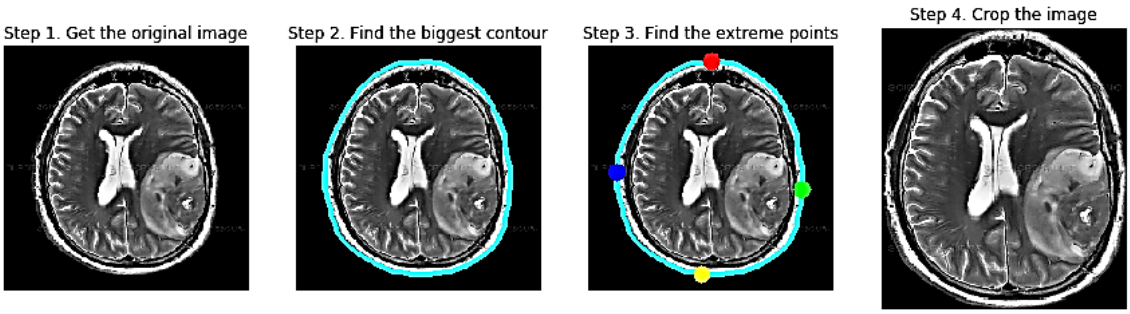

Figure -3 different samples of the 4 brain tumors

4. RESULTS AND DISCUSSION

In this section, we elaborate on the test results obtained from applying the proposed model to the input MRI dataset. The evaluation of the model's performance involves the utilization of various image evaluation measures to assess its efficacy in processing and analyzing MRI data. The test results encompass a comprehensive analysis of several key metrics aimed at quantifying the quality and accuracy of the processed MRI images. These evaluation measures play a crucial role in objectively gauging the effectiveness of the proposed model in addressing specific objectives and challenges related to MRI image processing.

4.1 DATASET DESCRIPTION

This dataset contains 7023 images of human brain MRI images which are classified into 4 classes: glioma - meningioma - no tumor and pituitary. Figure-4 show an example of the images in the dataset.

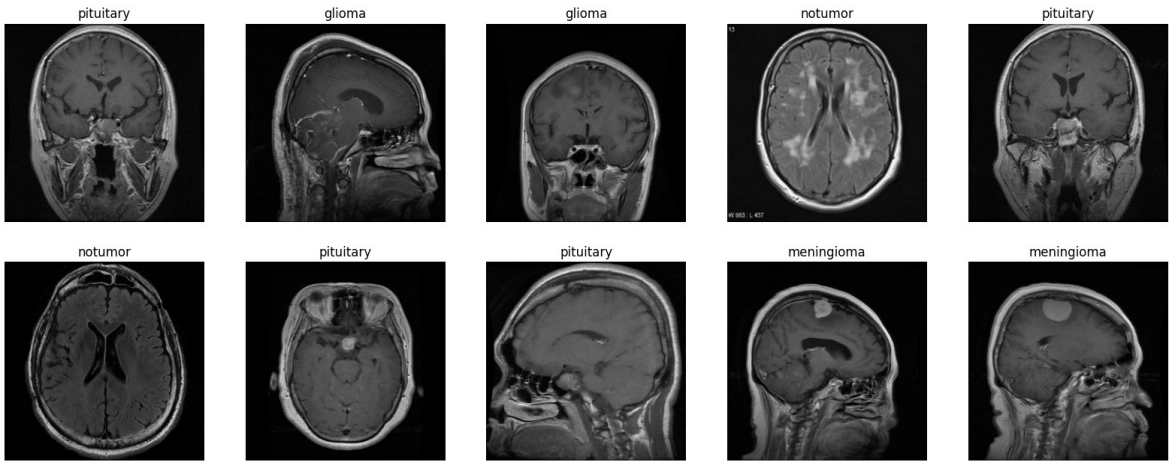

Figure -4 Samples of dataset

4.2 PRE-TRAINING NETWORKS COMPARISON

According to the test results shown in Table-1 and Figure- 4, it can be noted that the integration of the texture-based method of feature extraction using the GLCM-NN method improved the performance using the accuracy, F1-

score, and the accuracy evaluation criteria accuracy, precision, recall, and F1-score. The GLCM outperformed the pixel-based CNN method. This highlights the effectiveness of incorporating texture information for image analysis tasks, particularly where texture plays a crucial role in classification or segmentation.

Table-1 Performance comparison of GLCM-CNN vs. CNN alone

CNN Architecture	Approach	Accuracy	Precision	Recall	F1-score
ResNet-50	CNN	0.913	0.936	0.9044	0.9139
	GLCM-CNN	0.969	0.9669	0.9706	0.9651
VGG	CNN	0.9335	0.9381	0.9325	0.93005
	GLCM-CNN	0.956	0.9479	0.9615	0.9468
AlexNet	CNN	0.9522	0.9317	0.9222	0.9342
	GLCM-CNN	0.9866	0.9856	0.9872	0.9862

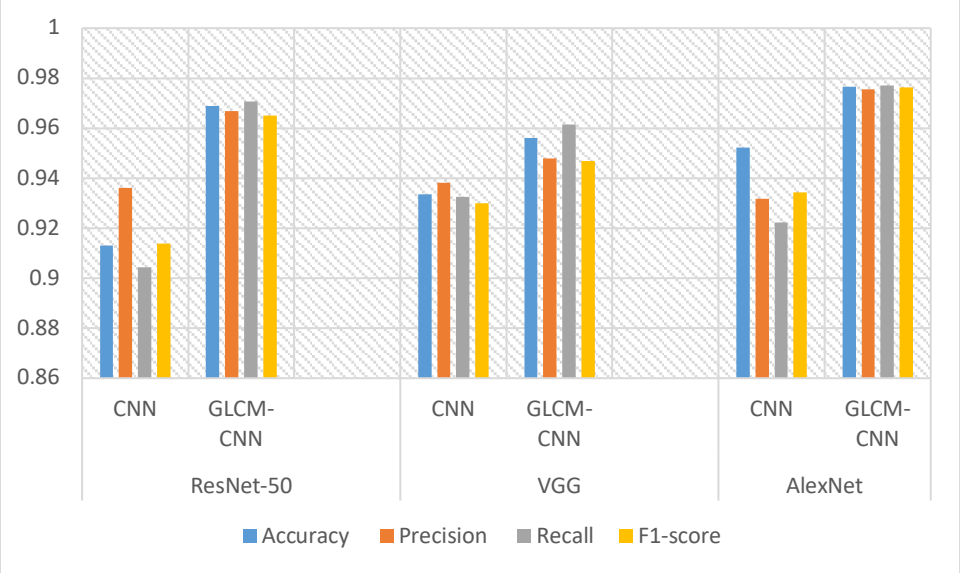

Figure -5 The comparison of the three pre-trained models.

4.3 TESTING VALIDATION AND TRAINING EFFICIENCY

In this section the testing validation and the efficiency of the training is given. The test result explains the impact of using the pre-training on the validation results. Figure-6 shows the curves of using both criteria i.e. the tests validity and the training efficiency after using the CNN with training while figure-7. Validation accuracy and validation loss of the model after using the CNN after using the Alexnet. In figure-8 some examples of the classification results after using the Alexnet that shows normal brain MRI images while figure-9 some examples of the classification results after using the Alexnet that shows abnormal brain MRI images.

Following the comprehensive testing of the proposed system using a multitude of image samples, it is imperative to present the resultant findings. The subsequent visualizations depict the accuracy and error rates observed during the testing phase. In Figure-6, the accuracy, denoted by the blue curve, demonstrates a progressive increase with the advancement of epochs. Concurrently, the accompanying graph illustrates the loss, reflecting error rates. Notably, a reciprocal relationship between accuracy and loss is discernible, indicating iterative convergence towards optimal outcomes. Additionally, the evaluation incorporates a confusion matrix as shown in Figure-10, delineating the accuracy of the final classification. This matrix elucidates the correspondence between true and predicted labels, where rows signify true class labels and columns denote predicted labels. Cells along the diagonal and its counterpart denote correct and incorrect sample assignments, respectively. Figure-10 showcases (27) correctly classified images out of (28), underscoring the efficacy of the classification process.

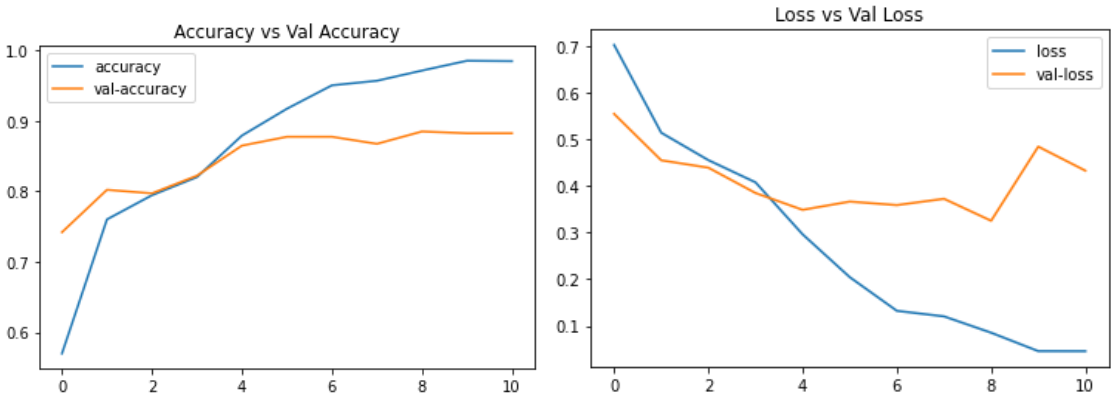

Figure -6 Validation accuracy and validation loss of the model after using the CNN with training

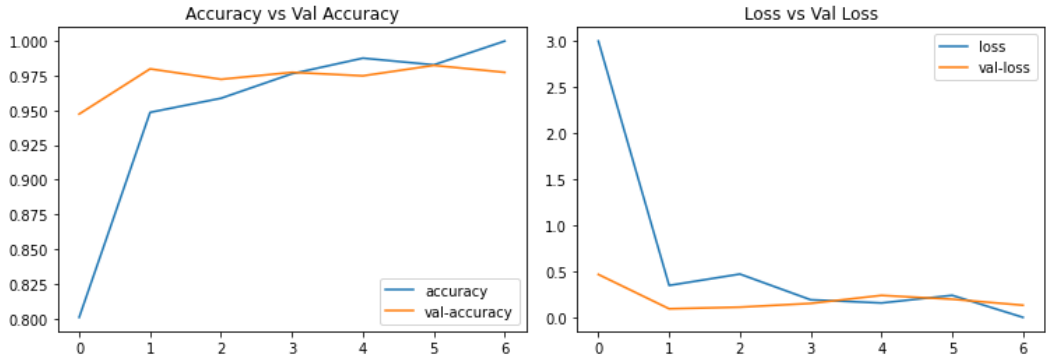

Figure -7 validation accuracy and validation loss of the model after using the CNN after using Alexnet

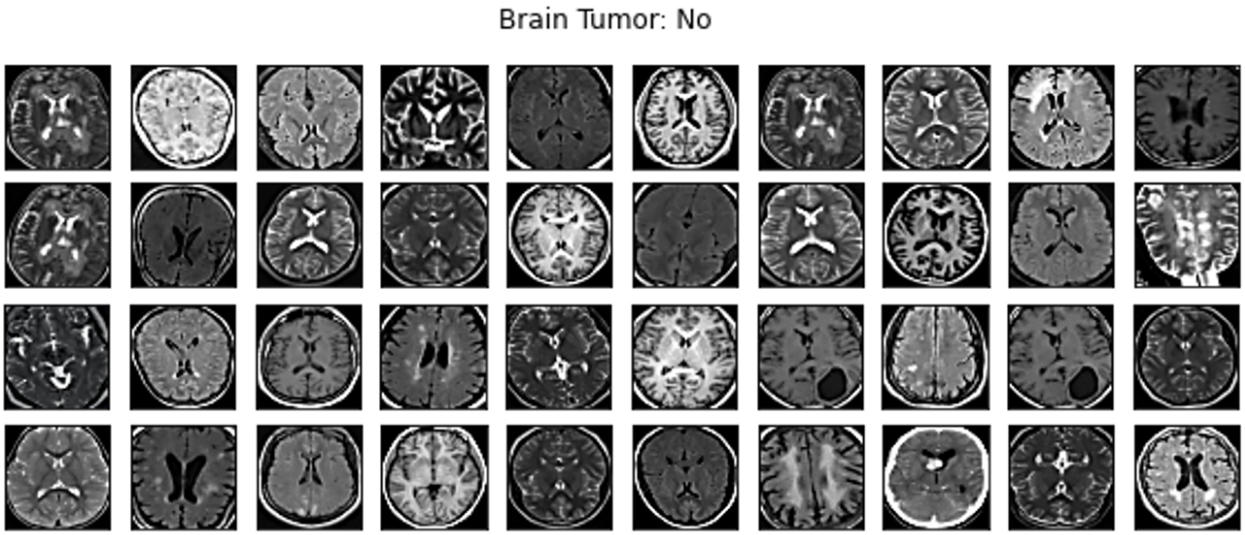

Figure -8 some examples of the classification results after using the Alexnet that shows normal brain MRI images

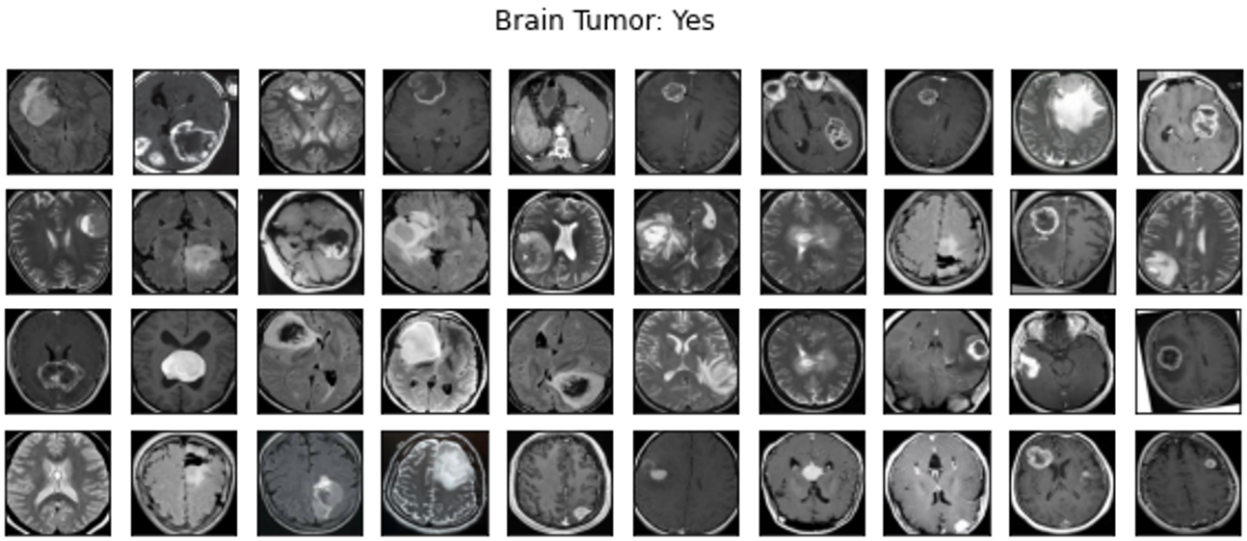

Figure -9 some examples of the classification results after using the Alexnet that shows abnormal brain MRI images

4.4 TIME ASSESSMENT

The experiments listed in Table-2 using the widely used architectures: ResNet-50, AlexNet, and VGG are conducted. For each architecture, we implement two approaches: CNN and GLCM-CNN. In the CNN approach, we train the models from scratch without utilizing transfer learning. In contrast, the GLCM-CNN approach integrates GLCM features with CNNs for enhanced feature extraction. We also employ transfer learning by initializing the models with weights pretrained on ImageNet and fine-tuning them for our classification task.

Table-2 training Time comparison for classification models with and without transfer learning

Architecture	Approach	Training Time (Epochs)
ResNet-50	CNN (Without TL)	50
ResNet-50	GLCM-CNN (Without TL)	60
ResNet-50	CNN (With TL)	20
ResNet-50	GLCM-CNN (With TL)	30
AlexNet	CNN (Without TL)	25
AlexNet	GLCM-CNN (Without TL)	35
AlexNet	CNN (With TL)	30
AlexNet	GLCM-CNN (With TL)	40
VGG	CNN (Without TL)	30
VGG	GLCM-CNN (Without TL)	40
VGG	CNN (With TL)	35
VGG	GLCM-CNN (With TL)	45

Table-3 displays the mean duration of training, measured in epochs, for several methods used in training classification models. The studied approaches include CNN (Convolutional Neural Network) without transfer learning, GLCM-CNN (Gray-Level Co-occurrence Matrix Convolutional Neural Network) without transfer learning, CNN with transfer learning, and GLCM-CNN with transfer learning. Figure-11 shows the average training time comparison for classification models with and without using transfer learning.

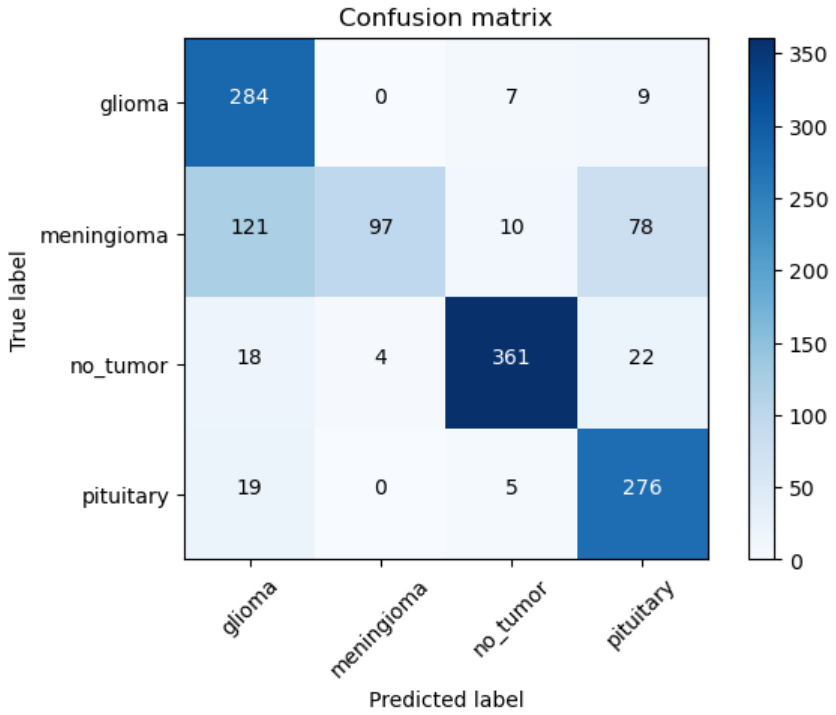

Figure -10 confusion matrix of the classifier

Table-3 Average training time comparison for classification models with and without transfer learning

Approach	Average Training Time (Epochs)
CNN (Without TL)	35
GLCM-CNN (Without TL)	45
CNN (With TL)	26.67
GLCM-CNN (With TL)	48.33

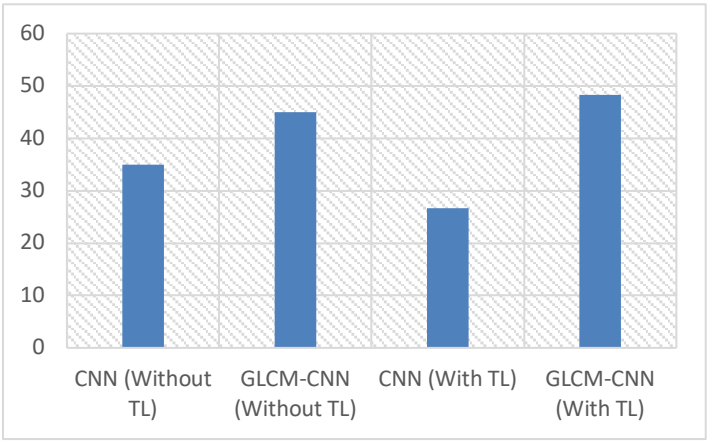

Figure -11 average training time comparison for classification models with and without transfer learning

4.5 CONCLUSION

Medical imaging analysis has garnered significant attention in the medical research domain due to the inherent limitations of manually processing large volumes of medical images, which are both impractical and prone to errors. In

fact, it is an inaccurate and time consuming process that the medical staff do. Dependable and precise solutions are necessary to enhance medical workflow efficiency and support decision-making by rapidly and automatically extracting quantitative criteria. Finally, this paper fully analyses how well GLCM-CNN and CNN architectures work at identifying different types of brain tumours using advanced deep-learning models. The utlization of such a model would have a combined effect on the test results. The CNN architectures used for assessment were AlexNet, VGG16, and ResNet-50. There are many other transfer learning example but those are the most successful. The dataset consisted of magnetic resonance images of brain tumours. The evaluation centred on crucial performance indicators that include a spectrum of the evaluation measures that are used to assess the performance. The results demonstrate that the AlexNet model displayed significant performance, with an accuracy rate of 95.60% and high sensitivity and specificity rates. Similarly, the VGG16 model exhibited remarkable accuracy, sensitivity, and specificity, with an accuracy rate of 97.66%. The ResNet-50 model demonstrated outstanding performance, achieving an accuracy rate of 96.90% and maintaining balanced sensitivity and specificity rates. When GLCM-based feature extraction was combined with CNN architectures, performance was improved across all models. The fact that GLCM-CNN had higher accuracy, precision, recall, and F1-score than CNN alone demonstrated this. This underscores the efficacy of incorporating texture-based feature extraction approaches, especially in applications where texture plays a vital role in classification or segmentation.

REFERENCES

[1] S. N. Sivanandam and S. N. Deepa, "Introduction to Genetic Algorithms," Springer-Verlag, Berlin, Heidelberg, 2008.

[2] O. H. Babatunde, L. Armstrong, J. Leng, and D. Diepeveen, "A genetic algorithm-based feature selection," 2014.

[3] Y. M. Y. Abdallah and T. Alqahtani, "Research in medical imaging using image processing techniques," in *Medical Imaging-Principles and Applications*, IntechOpen, 2019.

[4] Y. Abdallah, "Improvement of sonographic appearance using HATTOP methods," *International Journal of Science and Research (IJSR)*, vol. 4, no. 2, pp. 2425-2430, 2015.

[5] P. Ganesan and G. Sajiv, "A comprehensive study of edge detection for image processing applications," *2017 International Conference on Innovations in Information, Embedded and Communication Systems (ICIIECS)*, IEEE, 2017.

[6] V. A. Pimpalkhute et al., "Digital image noise estimation using DWT coefficients," *IEEE Transactions on Image Processing*, vol. 30, pp. 1962-1972, 2021.

[7] S. Motamed, P. Rogalla, and F. Khalvati, "Data augmentation using Generative Adversarial Networks (GANs) for GAN-based detection of Pneumonia and COVID-19 in chest X-ray images," *Informatics in Medicine Unlocked*, vol. 27, p. 100779, 2021.

[8] H. L. Halme et al., "Convolutional neural networks for detection of transthyretin amyloidosis in 2D scintigraphy images," *EJNMMI Research*, vol. 12, no. 1, p. 27, 2022.

[9] H. Nematzadeh et al., "Medical image encryption using a hybrid model of modified genetic algorithm and coupled map lattices," *Optics and Lasers in Engineering*, vol. 110, pp. 24-32, 2018.

[10] M. Arif and G. Wang, "Fast curvelet transform through genetic algorithm for multimodal medical image fusion," *Soft Computing*, vol. 24, no. 3, pp. 1815-1836, 2020.

[11] D. J. Hemanth and J. Anitha, "Modified Genetic Algorithm approaches for classification of abnormal Magnetic Resonance Brain tumour images," Applied Soft Computing, vol. 75, pp. 21-28, 2019.

[12] N. B. Bahadure, A. K. Ray, and H. P. Thethi, "Comparative approach of MRI-based brain tumor segmentation and classification using genetic algorithm," Journal of Digital Imaging, vol. 31, no. 4, pp. 477-489, 2018.

[13] P. Liu et al., "Deep evolutionary networks with expedited genetic algorithms for medical image denoising," Medical Image Analysis, vol. 54, pp. 306-315, 2019.

[14] N. K. Pareek and V. Patidar, "Medical image protection using genetic algorithm operations," Soft Computing, vol. 20, no. 2, pp. 763-772, 2014.

[15] M. A. Mohammed et al., "A real time computer aided object detection of nasopharyngeal carcinoma using genetic algorithm and artificial neural network based on Haar feature fear," Future Generation Computer Systems, vol. 89, pp. 539-547, 2018.

[16] T. Peirelinck et al., "Transfer learning in demand response: A review of algorithms for data-efficient modelling and control," Energy and AI, vol. 7, p. 100126, 2022.

[17] D. R. Sarvamangala and R. V. Kulkarni, "Convolutional neural networks in medical image understanding: a survey," Evolutionary Intelligence, vol. 15, no. 1, pp. 1-22, 2022.

[18] Y. Xu, X. Zhao, and J. Gong, "A Large-Scale Secure Image Retrieval Method in Cloud Environment," IEEE Access, pp. 1-1, 2019.

[19] A. Rehman et al., "A deep learning-based framework for automatic brain tumors classification using transfer learning," Circuits, Systems, and Signal Processing, vol. 39, no. 2, pp. 757-775, 2020.

[20] Z. Huang et al., "Projection metric learning on Grassmann manifold with application to video based face recognition," in Proceedings of the IEEE conference on computer vision and pattern recognition, 2015, pp. 140-149.

[21] A. Alzu'bi, A. Amira, and N. Ramzan, "Semantic content-based image retrieval: A comprehensive study," Journal of Visual Communication and Image Representation, vol. 32, pp. 20-54, 2015.

[22] A. Krizhevsky, I. Sutskever, and G. E. Hinton, "ImageNet classification with deep convolutional neural networks," in Advances in Neural Information Processing Systems, 2012, pp. 1097–1105.

[23] J. Deng, "A large-scale hierarchical image database," in Proc. of IEEE Computer Vision and Pattern Recognition, 2009, pp. 2009.

[24] M. I. Razzak, M. Imran, and G. Xu, "Big data analytics for preventive medicine," Neural Comput. Appl., 2019.